

# Evolution of subsea permafrost landscapes in Arctic Siberia since the Late Pleistocene: a synoptic insight from acoustic data of the Laptev Sea

P. Rekant<sup>1,6</sup> · H. A. Bauch<sup>2,5</sup> · T. Schwenk<sup>3</sup> · A. Portnov<sup>4</sup> · E. Gusev<sup>1</sup> · V. Spiess<sup>3</sup> · G. Cherkashov<sup>1,7</sup> · H. Kassens<sup>5</sup>

Received: 4 September 2015 / Accepted: 16 October 2015 / Published online: 20 November 2015  
© Springer-Verlag Berlin Heidelberg 2015

**Abstract** Using high-resolution seismic data, this study aims at investigating the evolution and morphological diversity of subsea permafrost features on the eastern Laptev Sea shelf, Arctic Siberia. Several seismic facies were recognized. These relate to the major environmental changes, which affected the Laptev Sea area before, during, and after the last global transgression. Because this shallow shelf was part of the Beringian landmass, we consider a prominent subsurface seismic basal reflector as the top of the former terrestrial permafrost table. Five zones differing in geometry, reflection patterns, depths, and continuity of the permafrost top are identified. Where visible, the upper 70 m of the sediments consists of epigenetically and syngenetically frozen ice-poor sandy deposits at the base, possibly of early last glacial age, marine isotope stages (MIS) 5 and 4. These are followed by late glacial, ice-rich facies interpreted to be MIS 3 to 2. The early Holocene (MIS 1) features well-stratified lagoonal and taberal deposits. As verified by radiocarbon-dated sediment cores, these deposits are overlain by middle to late Holocene sediments with an increasingly marine signature.

**Keywords** Arctic shelf · Laptev Sea · Subsea permafrost · High-resolution seismic

## Introduction

The Siberian Arctic seas (Laptev–East-Siberian–Chukchi seas) are vast shelf areas that are now covered by shallow waters. However, because the shelves break at around 100 m water depth, this region was part of the Beringian permafrost landscape that once connected Arctic Eurasia with the American continent during times of major glacial sea level lowstands.

Of these seas, the Laptev Sea shelf is one of the key sites where the existence of subsea permafrost was first suggested from bathymetry data [21, 22], geological onshore data [53], as well as mathematical modeling [20, 43–45, 58] assisted by deep, and shallow seismic studies [12, 29, 30] as well as near-coastal and offshore drilling attempts [18, 32, 36].

Purely mathematical modeling approaches would imply that major areas of the Laptev shelf are characterized by widespread ice-bearing and ice-bonded subsea permafrost, and so-called taliks, local areas of unfrozen ground within the permafrost. Judging on the onshore permafrost, the maximal thickness of the offshore permafrost is estimated to reach 500 m depending on the heat-flow values and lithology employed in the model [20, 45]. By contrast, direct evidence of the subsea permafrost is limited mainly to the shallow near-shore zone, whereas coast-distal information is still very sparse. Starting in the mid 1970s by Russian geological explorations, hundreds of boreholes were drilled offshore the Olenek and Khatanga interfluves, on the New Siberian Islands. These all documented as a subsea extension of the terrestrial permafrost (VNIIOkeangeologia internal reports).

---

✉ P. Rekant  
rekant@mail.ru

<sup>1</sup> VNIIOkeangeologia, Saint-Petersburg, Russia

<sup>2</sup> Mainz Academy c/o GEOMAR, Kiel, Germany

<sup>3</sup> University of Bremen, Bremen, Germany

<sup>4</sup> CAGE, University of Tromsø, Tromsø, Norway

<sup>5</sup> GEOMAR, Kiel, Germany

<sup>6</sup> VSEGEI, Saint-Petersburg, Russia

<sup>7</sup> Institute of Earth Sciences, St Petersburg State University, Saint-Petersburg, Russia

More recently, a number of Russian–German seismic and echosounder surveys to the eastern Laptev Sea discovered a basal reflector (BR), likely to be indicative for subsea permafrost [8, 12, 29, 30, 37]. However, the spatial distribution of the BR remained unclear. Coastal and offshore permafrost drilling campaigns were performed within the framework of the Russian–German Cooperation *Dynamics of Permafrost in the Laptev Sea* [6, 36]. These and other near-shore borehole profiles all discovered ice-bearing relict continental permafrost submerged under the sea. By comparison, offshore evidence for the existence subsea permafrost was revealed through offshore drilling in 2000 [18]. That study clearly shows that relicts of permafrost also exist today on the outer shelf and below a sediment cover of Holocene age [16].

Summarizing the above, we conclude that the existence of ground data about the regional offshore permafrost distribution is still insufficient and, therefore, knowledge remains rather elusive and speculative. Although the mathematical models predict widespread offshore permafrost, drilling observations so far provided only limited and very local information but lacked insight into the spatial distribution of subsea permafrost. It is the intention of this study to employ high-resolution seismic (HRS) data with the aim to give the first regional generalization of subsea permafrost distribution on the eastern Laptev Sea shelf. This research is based on the interpretation of a multitude of HRS lines which were collected during various ship campaigns between 1998 and 2006.

## Study area, dataset, and methods

The study area is located on the eastern Laptev Sea shelf at water depths of 15–60 m and between the Lena River delta and Kotel’ny Island (Fig. 1) within a subsea continuation of the North Yakutian coastal lowlands. The latter is an area of widely distributed Ice Complex (IC). The term IC is applied to permafrost sequences which usually consist of fine-grained, loess-like sediments with syngenetic ice wedges. On the northern Siberian lowlands, ICs formed during the Late Pleistocene regression (MIS 4-2), thus probably also including most of the drained Laptev Sea shelf. As these Siberian shelves remained largely unglaciated during the Late Pleistocene, sustained subaerial exposure led to the development of continuous permafrost hundreds of meters thick. This must have changed during Holocene inundation of the Arctic shelves, which ended at about 5–7 ka [3, 55], and during which air temperatures in the Arctic increased, also resulting in enhanced thawing of submerged permafrost [19].

Although this study is based on the complete HRS dataset available for the region at present (Fig. 1), data

quality significantly varied [29, 30, 34, 37, 39]. The best signal-to-noise ratio stems from seismic data acquired during Russian–German expedition “Transdrift-X” (TDR-X) in 2004. Thus, the initial seismic model is mainly based on that dataset. To verify and extrapolate the seismic model over a larger area of the eastern Laptev Sea shelf, both PARASOUND lines from Polarstern cruise ARK-XIV/Ib [17] and HRS data of Marine Arctic Geological Expedition (MAGE, Murmansk, Russia) [34] were also considered. Shipboard GPS navigation formed the basis for positioning, leaving an uncertainty on the order of a few tens of meters. The original bathymetric model was constructed by digitizing the large-scale nautical charts.

The TDR-X datasets were acquired by means of both “Sonic M-141” profiler system (VNIIOkeangeologia, Saint-Petersburg) and multichannel seismic (MCS) system of Bremen University, Germany [49]. Sonic M-141 comprises 4.5 kHz profiler and side-scan sonar mounted on the towed fish. MCS includes 48-channel streamer, BISON seismic recording system and a SODERA S-15 watergun. The seismic frequencies range from 100 to 500 Hz. Both “Sonic M-141” and MCS systems were operated simultaneously. The MCS system was towed at a distance of 100–150 m astern, whereas “Sonic M-141” was launched below the ship stem at a water depth of 6 m.

Since the main objective of the TDR-X cruise was to detect seismic signatures related to subsea permafrost, a number of seismic lines were acquired in scouting mode in order to select the most promising sites within the selected study area. Based on these scouting lines, the seismic survey focused near the SW foot of Semenovskaya bank at 15–39 m water depths (Fig. 1). A total of 42 HRS lines were obtained during TDR-X expedition, and 25 of them acquired from the TDR-X key area.

Seismic data were interpreted in “The Kingdom Suite” software (by Seismic Micro-Technology, Inc, Texas, USA) with routine seismic procedures for horizon identification, tracing, and mapping. Then all seismic horizons were exported into “Surfer” for 3-d imaging and spatial analysis.

## Results

### Seismic features

In this paper we describe permafrost-related seismic signatures and provide seismo-stratigraphic characteristics for HRS sections. The most prominent seismic feature found in the HRS data is a strong BR separating the lower acoustically transparent unit (ATU) from the upper stratified one. This boundary is a high-amplitude reflector with well-defined positive polarity, suggesting an increase in acoustic impedance (Fig. 2). Very often the BR looks like a non-

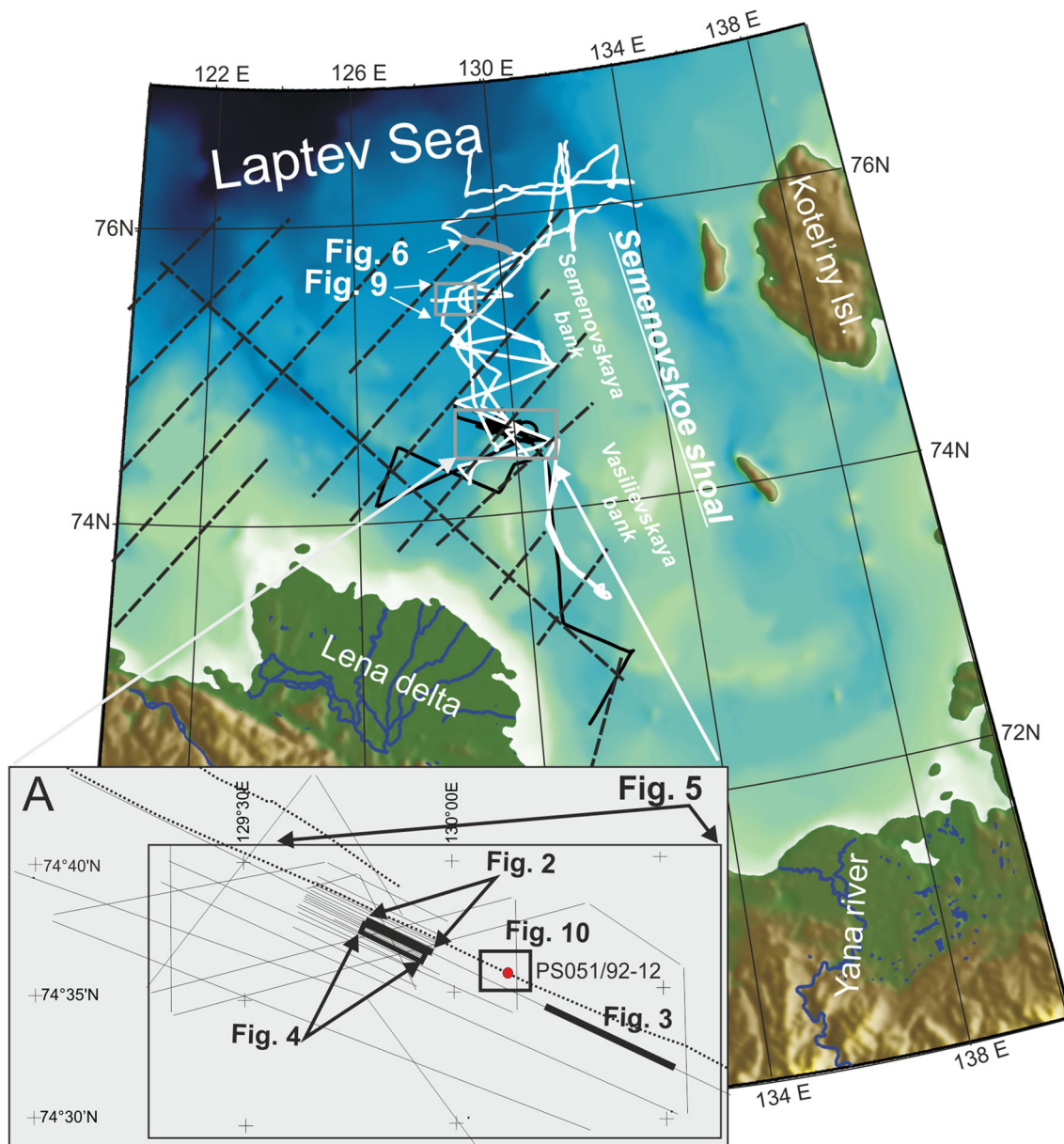


**Fig. 1** Location map of the study area in the Laptev Sea. White lines show PARASOUND profiles obtained during ARK-XIV/1b cruise [17]. Solid black lines indicate HRS profiles of survey TDR-X. Dashed black lines HRS lines of MAGE [34]. Inset A shows location of TDR-X key area. The bold lines show location of the figures in the text

upper one, marine sequence (see section “[Interpretation](#)”), overlies both fill sequence and acoustically transparent units in the depressions and on the highs, respectively (Fig. 2). A distinct lower reflector is observed in the lower part of fill sequence over the majority of depressions (Figs. 2, 3). The acoustic stratification is generally weakening upward in the seismic section.

stratigraphic, i.e., post-sedimentary, boundary, crosscutting the host strata. The BR occurs at the depths of 20 m below the sea floor (mbsf) in the central part of the TDR-X study area, but ascending up to 1 mbsf farther in the southeast (Fig. 3). In the central part, the BR forms a prominent hummocky surface with a number of flat, 0.5–6 km wide, highs and depressions with relative elevation changes of up to 20 m (Fig. 2e). In the remainder of the study area, the BR is more leveled and diffused.

The sediment pattern above BR is subdivided into two units by a subhorizontal top reflector. The lower one, named fill sequence, occurs only in depressions while the

The sea floor is characterized by V-shaped incisions 2–4 m deep and  $\leq 40$  m wide with one or two shoulders elevated above the adjacent seafloor (Fig. 2). We interpret these features as recent sea-ice ploughmarks, which were also evidenced from the side-scan sonar mosaics as linear,

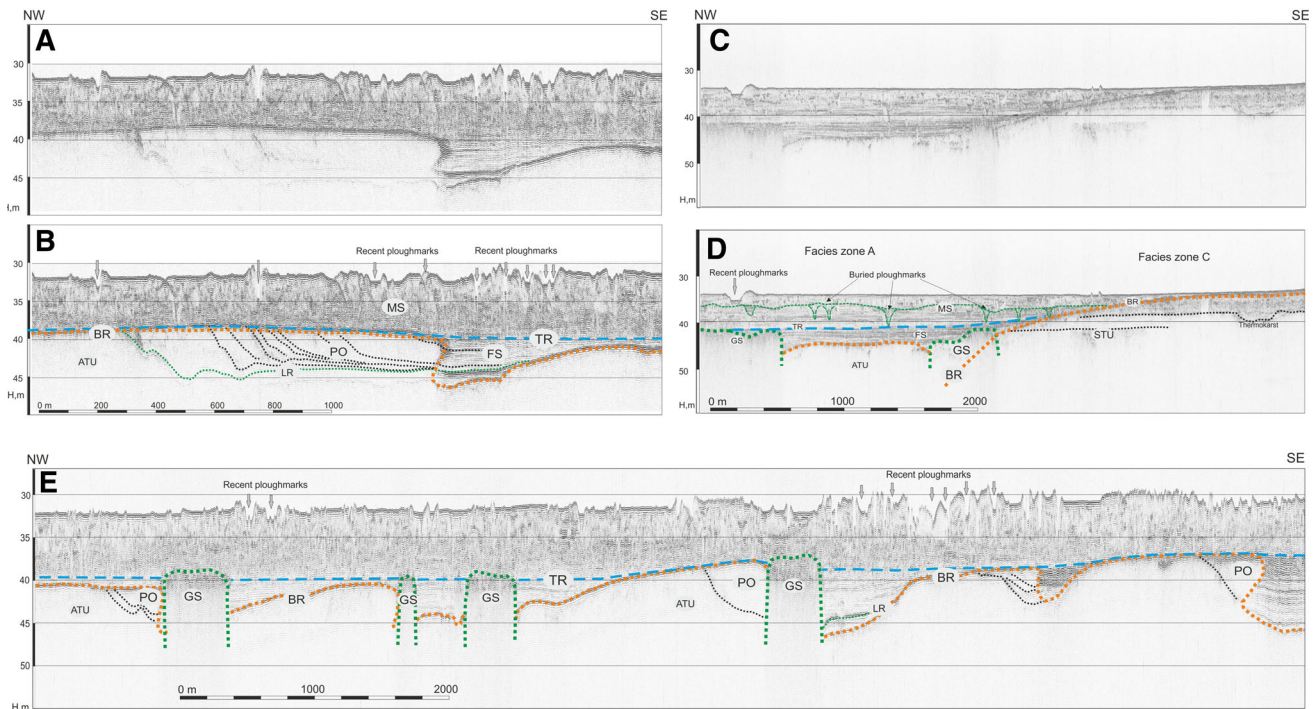


**Fig. 2** Fragments of the 4.5 kHz “Sonic-141” profiler lines S-035 (a) with interpretation (b) and S-011 (c) with interpretation (d) and S-040 with interpretation (e). Location of the lines is indicated in Fig. 1A. Basal reflector (BR) is clearly observed at the top of acoustically transparent unit (ATU). Stratified sediment sequence

above the BR is divided by the TR into the fill sequence (FS) and marine sequence (MS). The number of clinoforms occurred within permafrost overhangs (PO). Gas seeps (GS) appeared at the NW edges of the depressions. Other acronyms: LR lower reflector, STU semitransparent unit

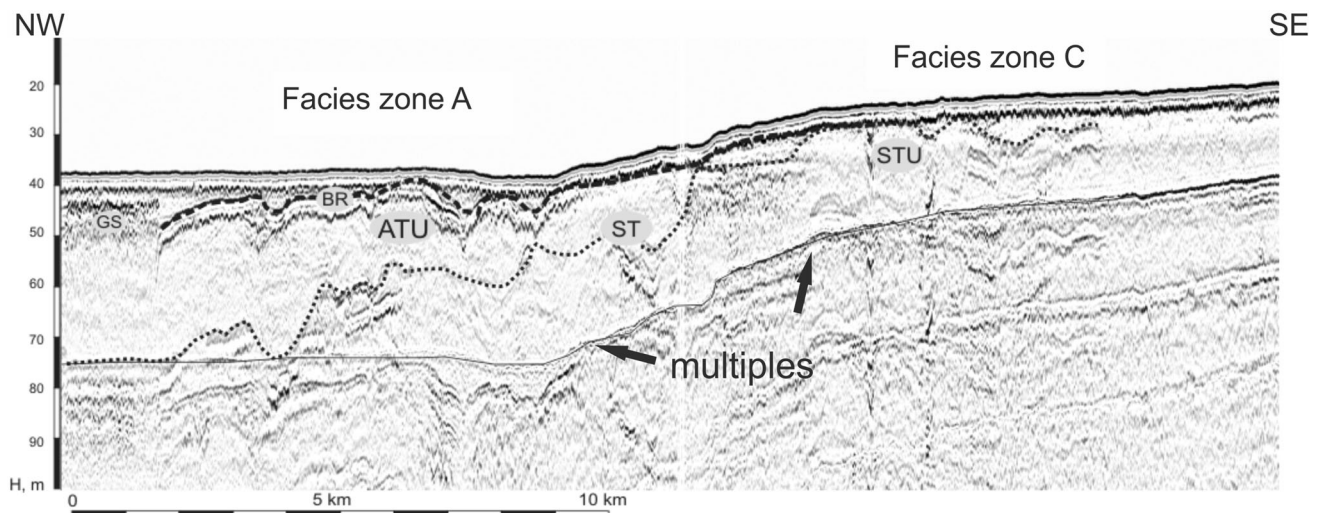


**Fig. 3** Seismic line GeoB04-011 of “BISON” seismic system shows the transition between facies zones A and C near Vasilievskaya bank. For location see Fig. 1A. Prominent seismic boundary with dissected topography marks the top of sands (ST). The semitransparent unit

(STU) revealed beneath the ST is assigned to the Muruktian sandy deposits. Other acronyms: LR lower reflector, ATU acoustically transparent unit, GS gas seeps

curvy-linear, and circular channels on the seafloor. Similar V-shape incisions, but filled with stratified sediments, are found on the HRS data (Fig. 2e) at depth of 3–5 mbsf. These featured are considered as an ancient, buried ploughmarks,

which become less abundant downward in seismic sections and completely disappearing at subbottom depths >5 m.

Fill sequences are notably asymmetric. Near the south-eastern parts of the depressions, they onlap acoustically

transparent deposits, whereas at the western and north-western side it forms a progradational stacking pattern with clinoforms (Figs. 2, 4). The clinoform package might indicate prevalence of sediment influx from the northwest of the depressions.

Remarkable transparent zones were discovered within a clinoform package at the NW edges of BR depressions (Fig. 2). As documented before [39], these zones can easily be traced across several parallel seismic lines headed both NW and SE directions (Fig. 5A). Therefore, we believe

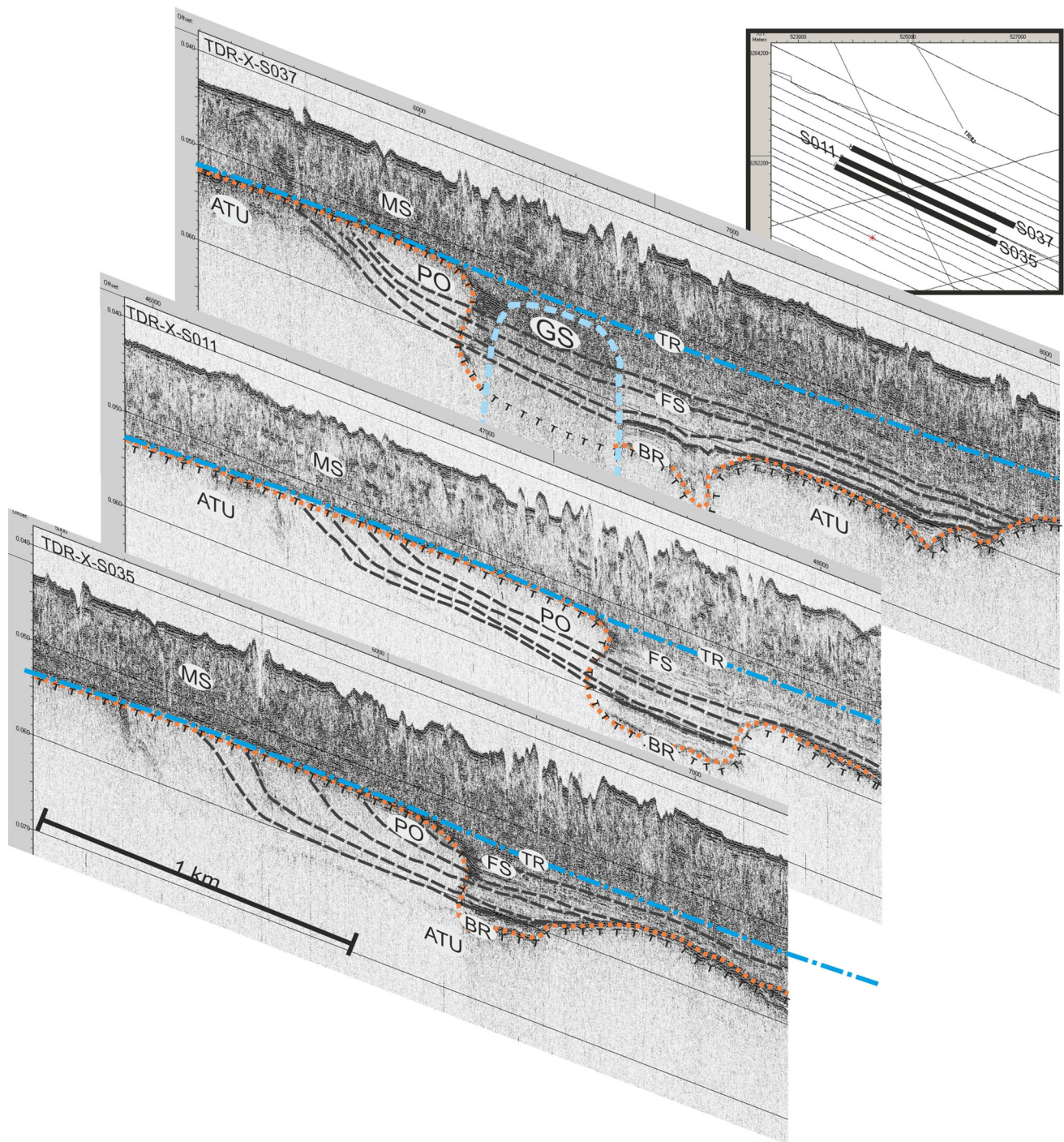


**Fig. 4** Fragments of the 4.5 kHz “Sonic-141” profiler lines # S-037, S-011, and S-035 with interpretation. For location see Fig. 1A. The package of the prograding clinoforms at the NW edge of depression is clearly defined within “permafrost overhung” (PO). *T-shape line*

marks the recent location of the acoustically defined permafrost table. Gas seeps (GS) associated with taliks [39]. Other acronyms: ATU acoustically transparent unit, FS fill sequence, MS marine sequence, TR top reflector

that these features do not represent seismic artifacts but features called “permafrost overhung” [2]. These forms are believed to originate from lateral freezing of lacustrine deposits under shallow water environments. Following that description, we adopted the name “permafrost overhung” for our found transparent zones [39].

A large number of vertical acoustic blanking anomalies with an uneven, degraded surface on top were found on the seismic records (Figs. 2, 4). Within the TDR-X key site, they commonly occur within centers of deeply buried BR depressions (Figs. 4, 5) and are therefore likely due to concentrated gas discharge. We interpret them as areas of concentrated gas seeps. Another type of gas discharge is revealed in the central part of the study area and within a former Lena paleovalley (Figs. 6, 7). Its seismic signature is rather pervasive being diffuse or “fuzzy” and shows neither an apparent interface below nor inner reflectors. Such extended areas of scattered gas seeps may therefore be associated with subsea permafrost degradation below a paleovalley.

**Sediment core features**

No deep drilling data are available from our key study area. However, the giant gravity core (kasten corer) PS51/92 was

taken from the eastern Lena paleovalley during Polarstern cruise in 1998. Radiocarbon dates show that the core’s chronology extends back to almost 9 ka (Fig. 8). Further analysis of geochemical features, which allow a distinction between terrestrial and marine organic matter ( $\delta^{13}C_{org}$ ), in combination with micropaleontological investigations all clearly indicate that sediments before 7.5 ka (i.e., the lowermost 2 m of the core) were deposited under low-salinity conditions, i.e., under the influence of terrestrial river runoff carrying terrestrial organic material with a typical terrestrial carbon signature.

Transferring the seismic information, downcore data, and chronology of site PS51/92 to nearby HRS line S-011/15 supports our notion made above (Fig. 8) that the infilled depressions, which are so well stratified, must reflect a type of sediment that was deposited under terrestrial, permafrost conditions.

**Interpretation**

Permafrost produces a rapid increase in the acoustic velocity of the seismic signal. A number of field and laboratory studies have shown that the P-wave velocity of ice-bearing coarse-grained sediments is strongly dependent on

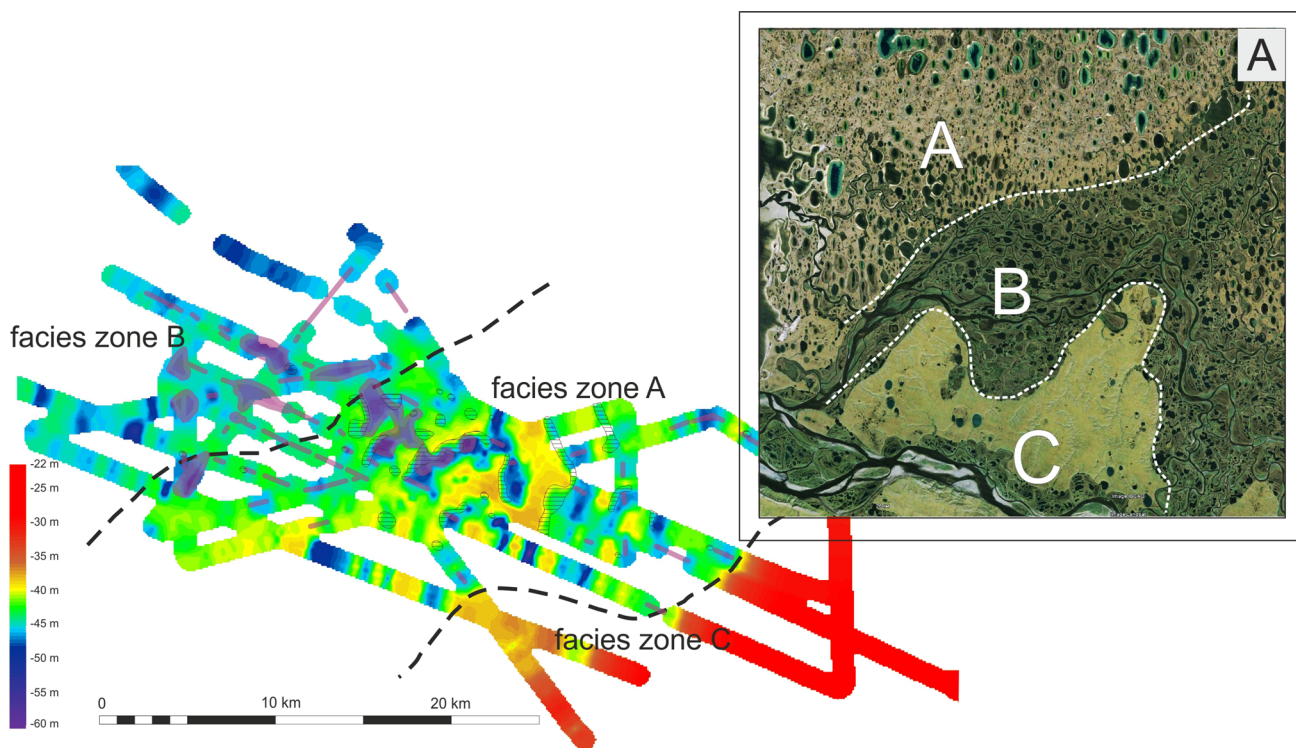


**Fig. 5** Topography of the BR surface, interpreted as a top of acoustically defined permafrost. For location see Fig. 1A. Depressions are believed to be of thermokarst origin. Gas seeps (pink) appear in the centers of thermokarst depressions and are associates with

taliks. The *hatched areas* along the west edges of the thermokarst depressions mark the permafrost overhung (PO) structures. Similar facies zones within Lena delta are shown on the *inset A*

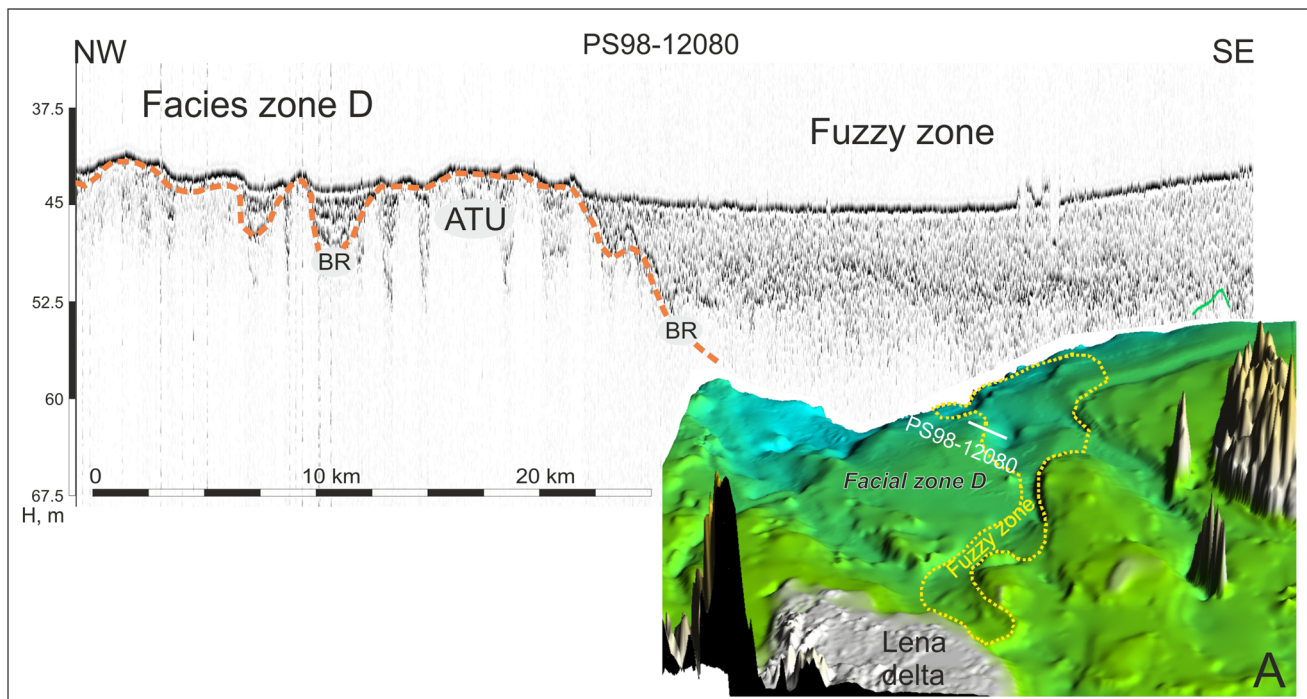


**Fig. 6** PARASOUND line PS98-12080 [17] in the eastern branch of Lena paleoriver valley (location is shown in Fig. 1). Obvious change of the seismic signature appears at the boundary between D and

“Fuzzy” facies zones. *Inset A* shows spatial distribution of the “Fuzzy” features. Other acronyms: *ATU* acoustically transparent unit

the ice content. The theoretical seismic velocities of 2.5–2.8 km/s for sands with 0–40 % ice content and from 3.4 to as high as 4.35 km/s for 40–100 % ice in pore space were determined by Johansen et al. [14]. Modeling experiments have shown an average velocity in unfrozen sediment strata of  $\sim 1.4$ – $1.8$  km/s, whereas the acoustic velocity in permafrost and frozen sediments rises up to 3.0–4.5 km/s [35, 41, 42]. This all causes significant change in the acoustic impedance at the interface between frozen and unfrozen deposits. In the HRS data, it normally shows as a prominent high-amplitude reflector with positive polarity. Thus, the top of a permafrost stratum can be distinguished from seismic records as prominent positive reflector. Because most of the PARASOUND data from the central Laptev Sea revealed a strong reflector at depths of 2–20 mbsf, this reflector was interpreted as the top of subsea permafrost [17, 37, 39]. A similar technique was used in a number of other studies on subsea permafrost [7, 31, 38, 40, 41].

Using all the information together, a total of five distinct facies zones were mapped in the study area. These differ in geometry of the BR, reflection patterns, depths, and continuity of the reflectors (Fig. 7).

*Facies zone A* occurs in the center of the study area west of Semenovskoe shoal (Fig. 7) and has peculiar BR features (Fig. 2). The BR is identified as high-amplitude non-

stratigraphic, i.e., post-sedimentary interface, which crosscuts the host reflectors and constrains a deeper penetration of the seismic signal. The hummocky topography of the BR within this zone is similar to the top of IC found in thermokarst-dominated terrains of the Yakutian lowlands [10, 11, 39, 50].

Therefore, we attribute this BR to the top of acoustically defined permafrost in the thermokarst-dominated terrain. As it was described earlier [50, 56], the thermokarst terrain was formed 13–12 ka and as a result of extensive thaw settlement of the top of the IC ice-rich deposits. Later on these features were filled with thawed structureless tabular deposits (i.e., permafrost sediments that thawed in a talik and then refroze). Modern remnants of such ice-rich deposits are ample on land, e.g., in the Lena Delta [25, 50–52]. At the beginning of the twentieth century, a few islands consisting of IC deposits still existed also on the southern Laptev Sea shelf [9, 15, 23]. These IC islands formed residual hills between the former branches of Lena and Yana paleoriver valleys and therefore were subject to intensive thermodenudation and wave erosion. Eventually they completely disappeared and turned into sandbanks with a modern water depth of  $\sim 5$ – $8$  m. The original bathymetric model, constructed by digitizing the large-scale nautical charts, provides new evidence for the existence of the IC remnants in the south of Laptev Sea. The

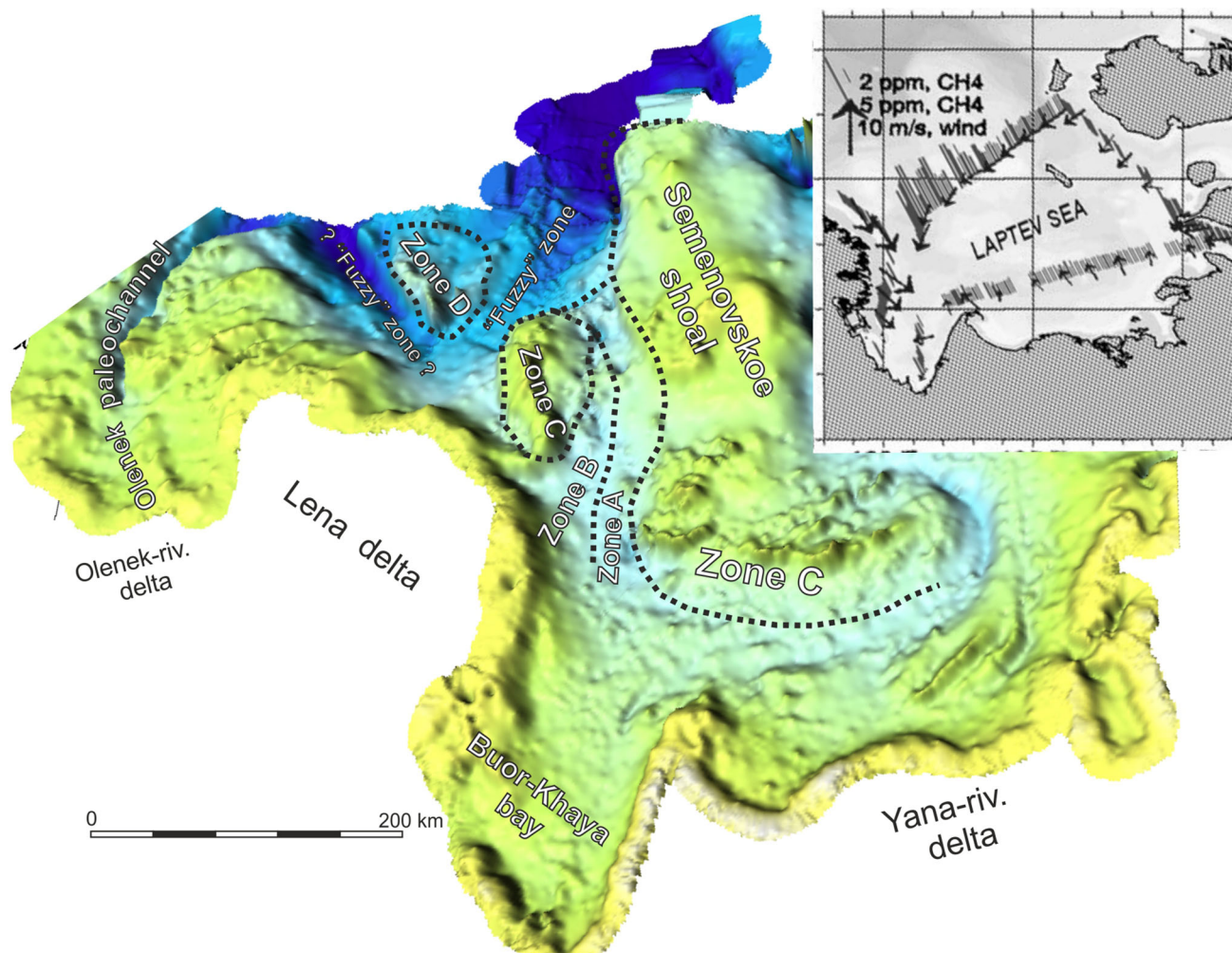


**Fig. 7** Map of the facies zones within the study area. The C, D and A, B facies zones are controlled by the local highs and terraces, respectively. The “fuzzy” zone in the pre-Lena paleovalley marks the area of extensive gas discharge caused by the permafrost degradation

pitted surface south of Semenovskoe shoal (Fig. 7) is supposed to be a bank formed recently at the place of the IC islands destroyed by the thermokarst processes.

The former existence of such IC remnants within the study area supports our assumption about the relation of the hummocky BR surface with the IC top. It also suggests that the deposits below the BR could be assigned to the Sartanian–Karginian IC deposits (correlative with MIS 3–2) of which the overlying sections (Fig. 2) are comprised of a fill sequence (uppermost Sartanian–early Holocene thermokarst deposits) and a marine sequence (middle and late Holocene transgressive deposits).

There seems to be a strong correlation between BR topography and “permafrost overhung” distribution, expressed in the development of a unified structure along the northwestern flanks of the BR depressions (Figs. 4, 5A). The basinward edges of the “permafrost overhung”

in the channel talik. The bathymetry is derived from digitizing of nautical charts. *Inset A* [46] shows an obvious increase in methane ratio in the atmospheric layer northeast of Lena Delta

are post-sedimentary boundaries, crosscutting, and partly blanking stratigraphic reflectors. This suggests that “permafrost overhung” resulted from bi-directional upward and downward freezing of lagoonal deposits. The occurring gas seeps mark zones of high sediment permeability, which are likely associated with taliks in the permafrost [39].

The narrow *facies zone B* is located northwestward of zone A (Fig. 7) and exhibits a fairly smooth topography of BR. It occurs at an average depth of 45 m below sea level. An ATU underlies the BR similarly to zone A, but the strength of this seismic boundary is slightly less. Thus, we suppose that the facies pattern within zone B is similar to those observed in facies zone A.

*Facies zone C* is outlined within Vasilievskaya and Semenovskaya banks and might be potentially found on similar shoals outside of the study area as well (Fig. 7). The sedimentary succession here differs strongly from



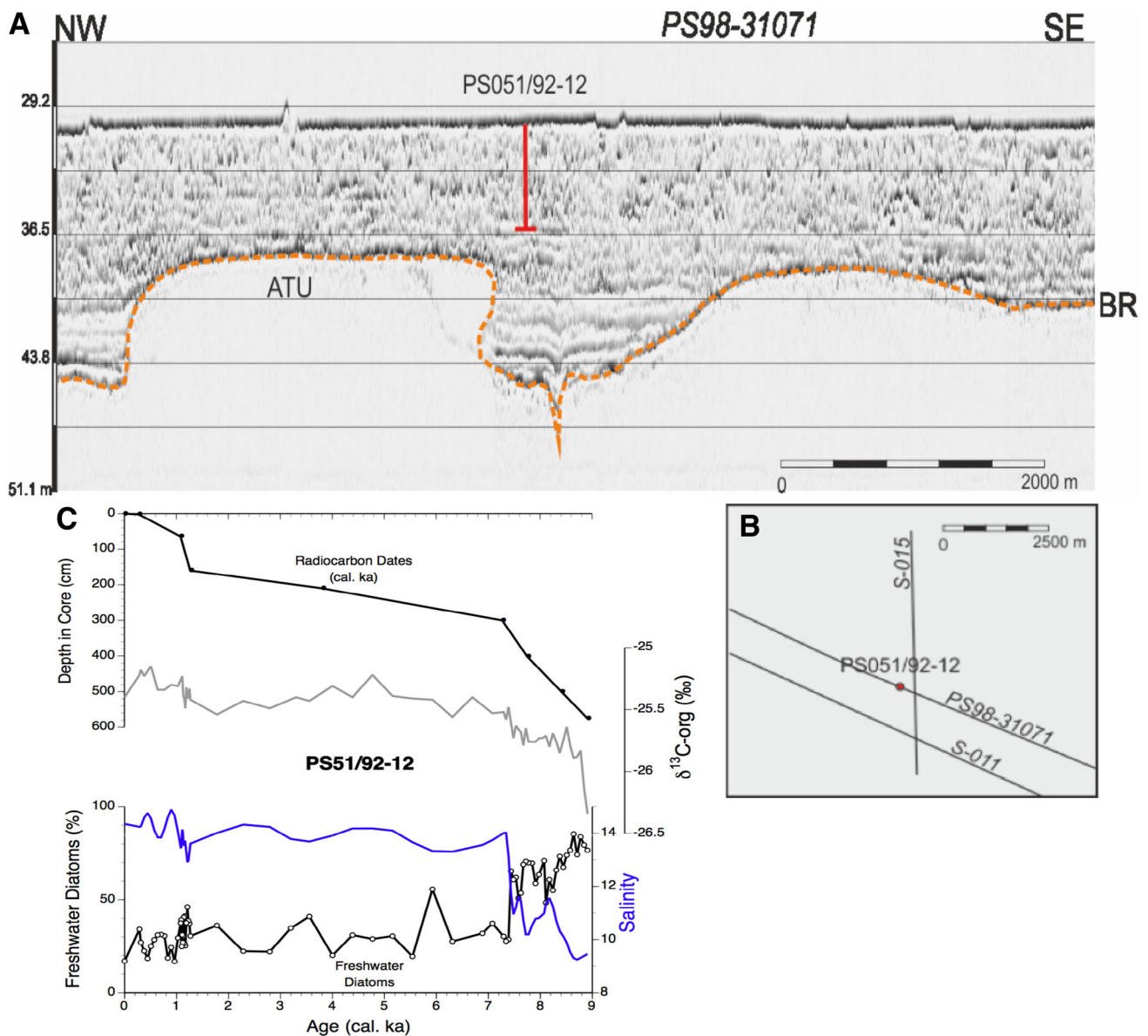


**Fig. 8** a PARASOUND acoustic section PS98-31071 showing the position and penetration of giant kasten corer PS51/92-12; **b** right inset indicates section track overview in the area (including nearby TRD-X S-011; see Fig. 10). **c** Stratigraphic length of PS51/92-12 and

sedimentation rates based on AMS-dated shell material [4]. The geochemical and micropaleontological data including salinity reconstructions clearly demonstrate the stepwise change in depositional environment after ca. 9 ka [5]

those described above. Flat and diffused BR occurs at depths of 1–5 mbsf. An ATU wedges out at the boundary between A and B zones. Due to this the underlying semi-transparent unit appeared just below BR (Fig. 3). Based on the weak reflectivity of the BR and seismic signature comprising short seismic reflectors remnants, we assign the latter to a degraded ice-bearing permafrost within sandy deposits.

A correlative sedimentary succession was found in and near the Lena Delta [11, 50] where ancient ice-poor sandy sediments discordantly underlay the ice-rich Karginian–Sartanian IC. The former are assigned to the Muruktian

ice-poor fluvial and/or alluvial sands [11, 25, 50]. However, reliable datings for this time interval [24, 50] are sparse and range from 88 to 37 ka. Based on this, the semi-transparent unit is considered to be pre-Karginian (pre-MIS-3, most probably Muruktian and uppermost Kazanian) ice-poor epigenetically frozen deposits [39].

*Facies zone D* comprises the hilly terrain in the north-western part of the area (Figs. 7, 9). This zone is characterized by hummocky sea floor topography and shallow bedding of the BR. Significantly weak seismic penetration is caused by an extremely high reflectivity of the BR. The latter occurs just below the seafloor on the highs overlain

by a very thin <math>\lt;2\text{--}3\text{ m}</math> sediment veneer. In the depressions it dips down to 10–15 mbsf. The BR topography is similar to the thermokarst surface within facies zone A, but now exposed to the sea floor. The phenomena of the occurrence of subsea permafrost right below the sea floor might be explained by permanent tectonic uplift of this zone followed by persistent denudation of the upper sediments.

“Fuzzy” facies zone occurs within the Lena paleovalley (Fig. 7). Seismic records from this zone exhibit a chaotic acoustic image with an uneven, “fuzzy” base interface. Such a seismic signature may be caused by widespread subsurface gas discharge, which totally obscures the internal seismic structure. Spatial distribution of the “fuzzy” anomalies (Fig. 7) shows that they follow the ancient river valleys on the shelf. Taking into account the results of modeling [44] and geochemical evidence of methane venting [46] as well as the HRS data, we attribute them with a linearly scattered gas escape zones caused by river taliks.

To summarize, all the observations allow us to identify four seismic units correlative to regional sedimentary successions (Table 1). Acoustically semi-transparent deposits, related to polygenetic pre-Karginian (most probably Muruktian–uppermost Kazanian) ice-poor sandy deposits, occur at the base of the seismic section. Within zones A and B, they are discordantly overlain by acoustically transparent deposits (interpreted here as Karginian–Sartanian IC) and are strongly affected by thermokarst. These thermokarst depressions are filled with tabular sediments (probably of Sartanian age) and succeeded by early Holocene lagoonal deposits. The transformation of the thermokarst depressions into lagoons and the subsequent accumulation of lagoonal deposits began as soon as the advancing sea had reached the study area. The continuing sea level rise and, with it, the southward migration of the Lena River mouth eventually led to the deposition of the middle to late Holocene marine sequences.

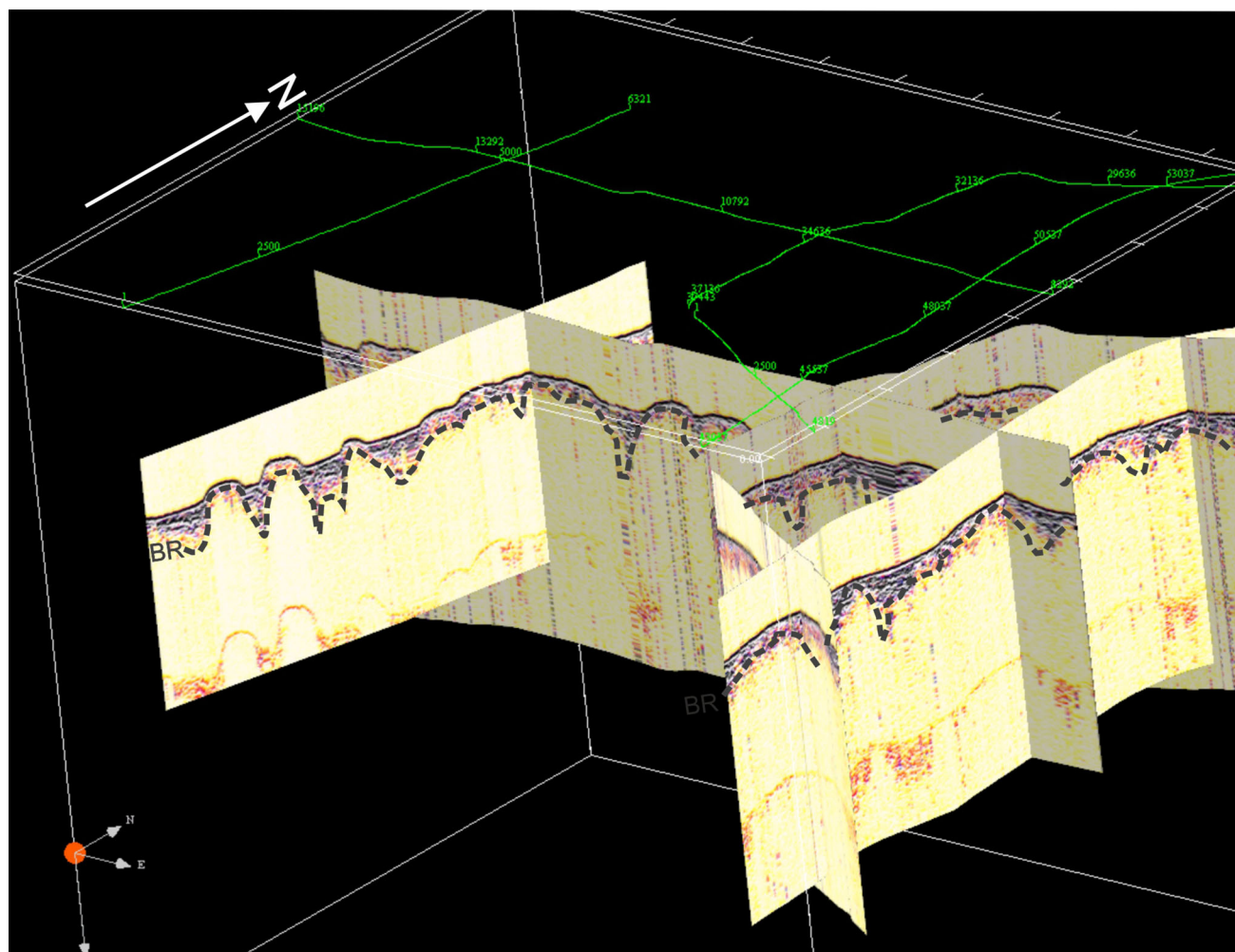


**Fig. 9** 3D sketch of the PARASOUND lines from cruise ARK-XIV/1b [17] within the facies zone D. The hummocky on the seafloor is caused by the BR topography. For location see Fig. 1

**Table 1** Overview of seismic features and interpretations

Seismic features	Seismic image	Location	Age interpretation
Marine sequence (MS)	Stratified at the bottom and acoustically disturbed at the top. Contains recent (surface incisions) and older (buried) ice ploughmarks	Entire study area except top of Semenovskoe shoal	Middle and late Holocene transgressive deposits
Permafrost overhung (PO)	Acoustically transparent zone within fill sequences. The NW edges are post-sedimentary in origin—crosscutting stratigraphic reflectors. The opposite onlaps ATU	Forms a unified structure along the northwestern flanks of BR depressions	Resulted from bi-directional (upward and downward) freezing of lagoonal deposits during Sartanian (MIS 2) regression
Fill sequence (FS)	Well-stratified seismic image. Lower reflector (LR) in the middle, top reflector (TR) above	Occurs only in depressions	Considered as uppermost Sartanian (MIS 2)—early Holocene thermokarst (lacustrine and lagoon) deposits
Basal reflector (BR)	Lowermost, high-amplitude reflector with well-defined positive polarity, suggesting an increase in acoustic impedance. Frequently as non-stratigraphic (post-sedimentary) boundary, crosscutting the host strata	Entire study area except top of Semenovskoe shoal	Indicative for subsea permafrost [8, 12, 29, 30, 37]
Acoustically transparent unit (ATU)	Transparent unit	Entire study area except top of Semenovskoe shoal	Interpreted as Karginian–Sartanian (MIS 3–2) Ice Complex
Semitransparent unit (STU)	Weak seismic reflector remnants	On the banks within Semenovskoe shoal. Lowermost seismic unit in HRS data	Pre-Karginian (pre-MIS-3, most probably Muruktian (MIS 4) and uppermost Kazanian (MIS 5e) ice-poor epigenetically frozen sands

The ploughmark incisions at the sea floor are the most recent features. According to Barnes and Reimnitz [1], such ice ploughmarks mainly form on Arctic shelves as a result of ice-scouring pack ice ridges in water depths between 10 and 50 m. Thus, the stratigraphic position of the buried ploughmarks may be indicative for the time when the transgressing sea reached the required water depth for their generation in the study area (Fig. 10).

### Paleoenvironmental reconstruction

It is quite obvious that a reliable paleoenvironmental reconstruction cannot be established using the seismic data only. A chronological attempt is therefore made to integrate the analyses of our HRS data with existing onshore paleoenvironmental information and conceptual models [11, 13, 24, 27, 44, 47, 48, 50, 57]. According to our stratigraphic sequence, we are able to distinguish between eight successive stages of offshore environmental evolution (see Fig. 11).

As is inferred from the HRS data showing the accumulation of the semi-transparent unit, the oldest stage of the landscape development may be as old as >80–37 ka (possibly uppermost Kazanian (?) to pre-Karginian/Muruktian). This unit may consist of epigenetically frozen marine deposits with syngenetically frozen terrestrial deposits on top (Fig. 11a).

During the following Karginian period (MIS 3), summer temperatures improved several times [13] causing thermoerosion of the sandy basements with only minor accumulation of syncryogenic deposits over the drained shelf. The Late Karginian (34–24 ka) was characterized by summer temperature still high enough for steppe species survival [13]. During the peak of the last glacial maximum, the Sartanian (24–15 ka), high aridity, and relatively low summer temperatures prevailed. Syngenetically frozen ice-rich deposits similar to those found onshore (Karginian–Sartanian IC) accumulated within terraces of the Lena and Yana paleovalleys and eventually formed acoustically transparent units (Fig. 11b).

During the first phase of deglaciation (~15–12.5 ka; Bølling/Allerød), extensive thermokarst processes are considered to be the leading landscape transformation factor [13], causing a rapid degradation of the IC landscape [44]. Thermokarst lakes occupied the recently formed depressions, and the lake water eventually accelerated thaw settlement rates. This led to the formation of a deeply dissected topography of the thermokarst terrain. The irregular BR surface marked this stage on the HRS records (Fig. 11c).

With the beginning of the Holocene the rising sea level led to the gradual inundation of most of the Laptev Sea shelf [3] and a southward retreat of coastlines and river mouths [26, 33, 54]. During this time of continuous retreat of shorelines and massive mobilization of terrestrial

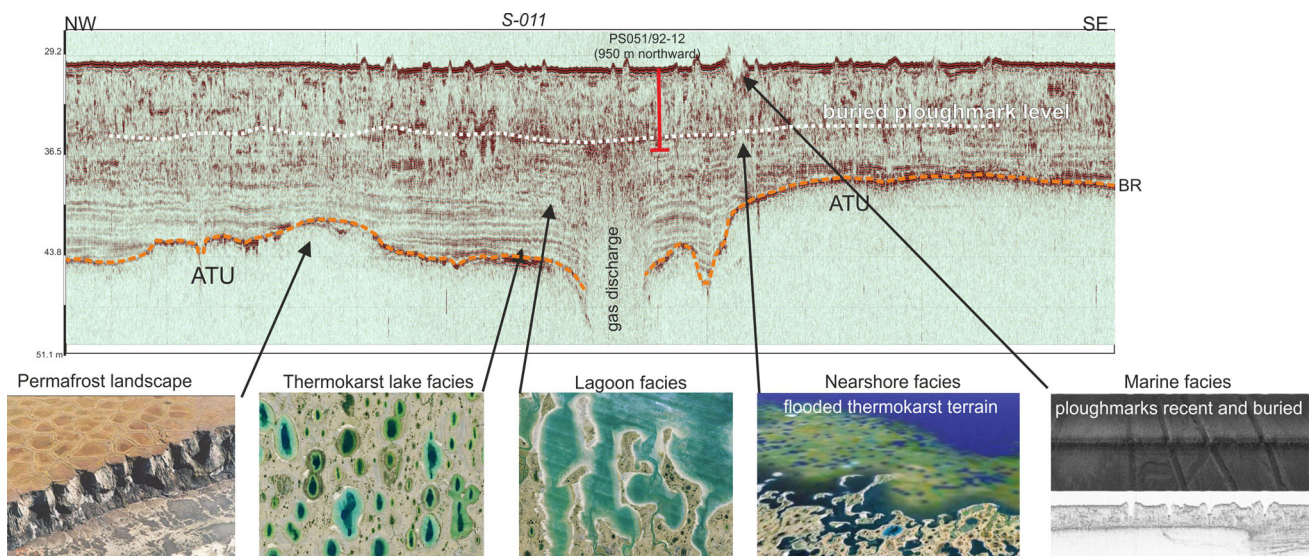


**Fig. 10** Major features of environmental changes as identified within the HRS data set of seismic line S-011, nearby core site PS51/92 (see Fig. 8). Other acronyms: ATU acoustically transparent unit

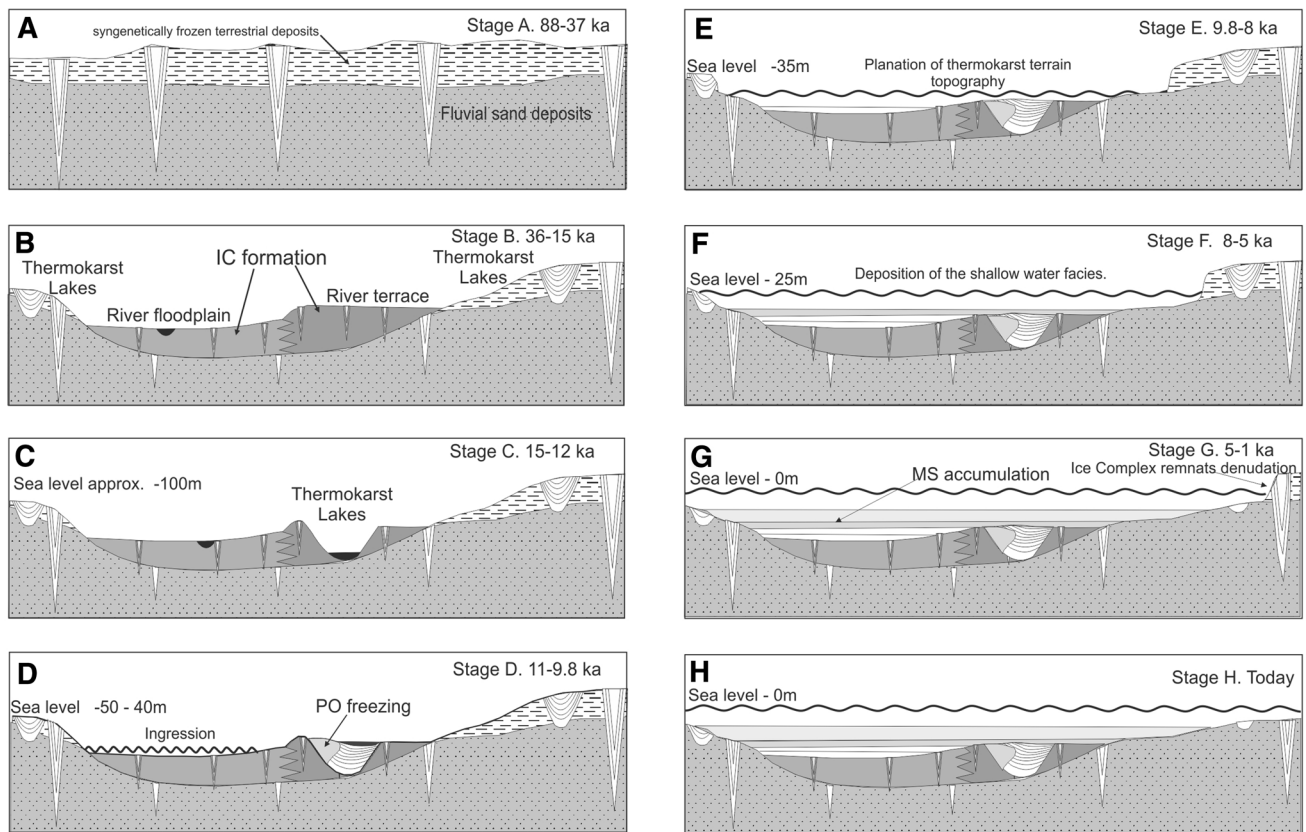


**Fig. 11** A schematic reconstruction of paleoenvironmental permafrost landscape changes over the eastern Laptev Sea shelf

permafrost sediments on the shelf [28], thermokarst lakes and alases were transformed into lagoons. Fostered by high air temperatures in the Arctic [19] thermoerosion processes accelerated landscape leveling, transporting the deposits

down the slopes where they accumulated in the nearby lake/ alas depressions. This stage is presented on the HRS records as a well-stratified fill sequence, leaving a rather flattened topography (Fig. 11d).

According to the sea level reconstruction, the mid-shelf region with water depths  $\sim 35\text{--}40$  m was flooded  $\sim 9.8\text{--}8$  ka [3]. It provides the time constraint for the flooding of the TDR-X key site, including that of core PS51/92 (Fig. 10). The landward advance of the shoreline resulted in transformation of the onshore permafrost terrain into marine shoals accompanied by enhanced high-wave erosion (Fig. 11e). Minor positive relief forms were finally denudated, while lakes and lagoons were completely filled with sediments. On the seismic record, this geological event is reflected as a prominent top reflector (TR on the Fig. 2) and so typical for the central part of the study area.

Depending on water depth, the final stage of sea level rise (8–5 ka) was marked by modern shallow marine sedimentation developed (Fig. 10). Since no ploughmarks were observed on the HRS data within the lower part of the marine sequence (see Fig. 10), we suggest that water depth in the TDR-X key site did not exceed 10 m at 8 ka (Figs. 10, 11f). The sea level reached its modern position  $\sim 6\text{--}5$  ka [3]. At that time shallow water stage F changed to marine stage G, providing typical marine depositional conditions over the study area (Figs. 8, 11g). As inferred from the HRS data, the transition from stage F to stage G is marked by frequent ploughmark activity (Fig. 11g).

Since then, thermal as well as sea-ice and wave-generated erosion caused a gradual disappearance of IC islands (Fig. 11h). Once the erosion front reached the top of the ice-poor sandy deposits, erosion rate significantly decreased and the former IC uplands were turned into subsea banks covered with sandy deposits.

## Conclusions

Five seismic facies related to the evolution of subsea permafrost are documented using HRS data from the eastern Laptev Sea shelf. A prominent BR is interpreted as a top of acoustically identified permafrost. In places the topography of the BR bears resemblance with present-day onshore thermokarst terrain. Four seismic units inferred from the HRS data fit well with existing paleoenvironmental models for the region [11, 13, 24, 27, 44, 47, 48, 50, 57]. An acoustically semi-transparent unit at the base of the seismic sections may represent the pre-Karginian (most probably Muruktian–uppermost Kazanian) epigenetically and syngenetically frozen ice-poor sandy deposits. The latter are discordantly overlain by acoustically transparent deposits assigned as the Karginian–Sartanian ice-rich IC. The thermokarst depressions on the top of the IC are filled with lacustrine to lagoonal sediments concordantly overlain by well-stratified marine sequence.

The HRS data also revealed abundance of the gas seeps in the study area. Most of them mark the local permeable zones within the permafrost, which are most likely former

thermokarst depressions (lakes/taliks). The “fuzzy”-facies of the gas seep anomalies are concentrated along the Lena and Yana paleoriver valleys and therefore may relate to river taliks.

Our seismic data also would indicate that the thermokarst terrain is exposed on the seafloor in the central part of the Laptev Sea shelf. This may originate either from the persistent denudation of the upper sediments due to the uplift of the region, or from a more recent destruction of formerly frozen sandy islands similar to Semenovsky and Vasilievsky.

**Acknowledgments** The research was carried under the Russian–German umbrella “Laptev Sea System” and within project “Permafrost” funded by the German Ministry of Education and Science (Grant 03G0589D), INTAS grant “Arctic environments: the protected areas of the Lena Delta and New Siberian islands—past and present development” (INTAS ref. 03-51-6682), Otto Schmidt Laboratory grant (OSL-06-20), and RFBR Grant 15-05-08497. The used software for interpretation of the seismic data (The Kingdom Suite 2d/3dPAK, version 8.2 by Seismic Micro-Technology, Inc, Texas, USA) was obtained as a University Gift Program grant. Comments by two reviewers help to improve the manuscript and are gratefully acknowledged.

## References

- Barnes PW, Reimnitz R (1997) Morphology and stratigraphy related to the nearshore boundary of the Stamukhi zone. In: Davies TA et al (eds) *Glaciated continental Margins. An atlas of acoustic images*. Chapman & Hall, London, pp 222–223
- Bases of Geocryology (1996) *Lithigenetic geocryology*, vol 2. MSU, Moscow (**in Russian**)
- Bauch HA, Mueller-Lupp T, Taldenkova E, Spielhagen RF, Kassens H, Grootes PM, Thiede J, Heinemeier J, Petryashov VV (2001) Chronology of the Holocene transgression at the North Siberian margin. *Glob Planet Change* 31:125–139
- Bauch HA, Polyakova YI (2003) Diatom-inferred salinity records from the Arctic Siberian margin: implications for fluvial runoff patterns during the Holocene. *Paleoceanography* 18(2):1027. doi:[10.1029/2002PA000847](https://doi.org/10.1029/2002PA000847)
- Bauch HA, Kassens H, Thiede J (2009) Transformation processes of the North Eurasian shelf environment since the last glaciation. In: Kassens H, Lisitzin AP, Thiede J, Polyakova YI, Timokhov LA, Frolov IE (eds) *System of the Laptev Sea and the adjacent Arctic Seas: modern environments and history of development*. MSU Press, Moscow, pp 373–383 (**in Russian**)
- Bolshiyarov DYu, Makarov AS, Gusev EA, Schneider W (2008) Problems of ice complex origination and former “Sannikovs Lands” existence in the Laptev Sea. *Problemy Arktiki i Antarktiki* 1:151–160
- Brothers DS, Ruppel C, Kluesner JW, ten Brink US, Chaytor JD, Hill JC, Andrews BD, Flores C (2014) Seabed fluid expulsion along upper slope and outer shelf of the U.S. Atlantic continental margin. *Geophys Res Lett*. doi:[10.1002/2013GL058048](https://doi.org/10.1002/2013GL058048)
- Delisle G (2000) Temporal variability of subsea permafrost and gas hydrate occurrences as function of climate change in the Laptev Sea, Siberia. *Polarforschung* 68:221–225
- Ermolaev MM (1932) The history of the discovery of New Siberian Islands, their study, and island trades. In: *Trudy Soveta po izucheniyu Proizvoditel'nykh sil, Ser. Yakutskaya* 7:9–38 (**in Russian**)
- Grosse G, Schirrmeyer L, Malthus TJ (2006) Application of Landsat-7 satellite data and a DEM for the quantification of

- thermokarst-affected terrain types in the periglacial Lena–Anabar coastal lowland. *Polar Res* 25:51–67
11. Grosse G, Schirmer L, Siegert C, Kunitsky V, Slagoda E, Andreev A, Dereviagin A (2007) Geological and geomorphological evolution of a sedimentary periglacial landscape in Northeast Siberia during the Late Quaternary. *Geomorphology* 86:25–51
  12. Hinz K, Delisle G, Block M (1998) Seismic evidence for the depth extent of permafrost in shelf sediments of the Laptev Sea, Russian Arctic? In: Proceedings of 7th international conference on permafrost, 23–27 June, 1998. Yellowknife, Canada, pp 453–458
  13. Hubberten H-W, Andreev A, Astakhov VI, Demidov I, Dowdeswell JA, Henriksen M, Hjort C, Houmark-Nielsen M, Jakobsson M, Larsen E, Lunkka JP, Lysa A, Mangerud J, Moller P, Saarnisto M, Schirmer L, Sher AV, Siegert C, Siegert MJ, Svendsen JI (2004) The periglacial climate and environment in northern Eurasia during the last glaciation (LGM). *Quatern Sci Rev* 23:1333–1357
  14. Johansen TA, Digraanes P, van Schaack M, Lonne I (2003) Seismic mapping and modeling of near-surface sediments in polar areas. *Geophysics* 68(2):1–8
  15. Karelin DB (1946) Final search of the Sannikov Land. *Izvestiya vsesoyuznogo geograficheskogo obschestva* 78:357–358 (in Russian)
  16. Kassens H, Thiede J, Bauch HA, Hoesemann JA, Dmitrenko I, Pivovarov S, Priamikov S, Timokhov L, Wegner C (2007) The Laptev Sea system since the last glacial. In: Harff J, Hay WW, Tetzlaff DM (eds) *Coastline changes: interrelation of climate and geological processes*. Geological Society of America, Special paper 426, 89–96
  17. Kassens H, Niessen F (2004) Profile of sediment echo sounding during cruise ARK-XIV/1b with links to ParaSound data files, Alfred Wegener Institute for Polar and Marine Research, Bremerhaven, PANGAEA. doi:10.1594/PANGAEA.141225
  18. Kassens H, Bauch HA, Dmitrenko I, Drachev S, Grikurov G, Thiede J, Tuschling K (2001) Transdrift VIII: drilling the Laptev Sea 2000. *Nansen Icebreaker* 12(1):8–9
  19. Kaufman Darrell S, Schneider David P, McKay Nicholas P, Ammann Caspar M, Bradley Raymond S, Briffa Keith R, Miller Gifford H et al (2009) Recent warming reverses long-term Arctic cooling. *Science* 325(5945):1236–1239. doi:10.1126/science.1173983
  20. Kholodov AL, Ryvkina EM, Gilichinskiy DA, Fedorov-Davydov DG, Gubin SV, Sorokovnikov VA, Ostroumov VE, Maksimovich SV (2003) Estimation of the organic carbon input into Arctic ocean due to erosion of Laptev and East Siberian seashore. *Earth's Cryosphere* 7(3):3–12
  21. Kluev EV (1965) Role in the dynamics of permafrost terrain factors of the polar seas. *Oceanology* 5:863–869
  22. Kluev EV (1966) Thermokarst manifestation at the bottom of the Laptev Sea. *Problemy Arktiki i Antarktiki* 23:26–32 (in Russian)
  23. Kordikov AA (1952) Laptev Sea sediments. Leningrad (in Russian)
  24. Krbetschek MR, Gonser G, Schwamborn G (2000) Luminescence dating results on sediment sequences of the Lena Delta. *Polarforschung* 70:83–88
  25. Kunitsky VV (1989) Cryolithozone of the Lena river lower part. Yakutsk (in Russian)
  26. Matul AG, Khusid TA, Mukhina VV, Chekhovskaya MP, Safarova SA (2007) Recent and Late Holocene environments on the southeastern shelf of the Laptev Sea as inferred from microfossil data. *Oceanology* 47(1):80–90
  27. Meyer H, Dereviagin AY, Siegert C, Hubberten H-W (2002) Paleoclimate studies on Bykovsky Peninsula, North Siberia—hydrogen and oxygen isotopes in ground ice. *Polarforschung* 70:37–51
  28. Mueller-Lupp T, Bauch HA, Erlenkeuser H, Hefter J, Kassens H, Thiede J (2000) Changes in the deposition of terrestrial organic matter on the Laptev Sea shelf during the Holocene: evidence from stable carbon isotopes. *Int J Earth Sci* 89(3):563–568
  29. Niessen F (2004a) Profile of sediment echo sounding during cruise ARK-IX/4 with links to ParaSound data files, Alfred Wegener Institute for Polar and Marine Research, Bremerhaven, PANGAEA. doi:10.1594/PANGAEA.206530
  30. Niessen F (2004b) Profile of sediment echo sounding during cruise ARK-XI/1 with links to ParaSound data files, Alfred Wegener Institute for Polar and Marine Research, Bremerhaven, PANGAEA. doi:10.1594/PANGAEA.206531
  31. Niessen F, Gierlich A, Weigelt E, Jokat W (1999) High-resolution seismic and sediment echosounding investigation of submarine permafrost on the Laptev Sea shelf. In: Proceedings of the fifth workshop on Russian–German Cooperation: Laptev Sea System, St. Petersburg, p 47
  32. Overduin P, Paul P, Liebner S, Knoblauch C, Günther F, Wetterich S, Schirmer L, Hubberten H-W, Grigoriev MN (2015) Methane oxidation following submarine permafrost degradation: measurements from a central Laptev Sea shelf borehole. *J Geophys Res Biogeosci* 120(5). doi:10.1002/2014JG002862
  33. Polyakova YI, Bauch HA, Klyuvitkina TS (2005) Early to middle Holocene changes in Laptev Sea water masses deduced from diatom and aquatic palynomorph assemblages. *Glob Planet Change* 48:208–222
  34. Proskurnin V, Shkarubo S (eds) (2014) State Geological map of Russian Federation. 1:1,000,000 scale. Sheet S-50—Ust'-Olenek. Explanatory note. SPb. VSEGEI (in Russian)
  35. Pullan S, MacAulay HA, Hunter JAM, Good RL, Gagne RM, Burns RA (1987) Permafrost distribution determined from seismic refraction. In: *Geology and geophysics. Marine Science Atlas of the Beaufort Sea*. Geological Survey of Canada. Miscellaneous Report 40. ISBN 0-660-53107-0. 37
  36. Rachold V, Bolshiyarov D, Grigoriev M, Hubberten H-W, Junker R, Kunitskiy V, Merker F, Overduin P, Schneider W (2007) Nearshore Arctic subsea permafrost in transition. *EOS* 88:149–156
  37. Rachor E (ed) (1997) Scientific Cruise Report of the Arctic Expedition ARK-XI/1 of the RV Polarstern in 1995. *Berichte zur Polarforschung*, 226, p 330
  38. Rekant P, Cherkashev G, Vanstein B, Krinitsky P (2005) Submarine permafrost in the nearshore zone of the southwestern Kara Sea. *Geo-Mar Lett* 25:183–189
  39. Rekant P, Tumskoi V, Gusev E, Schwenk T, Spiess F, Cherkashev G, Kassens H (2009) Distribution and peculiarity of subsea permafrost near Semenokoe and Vasilievskoe shoals (Laptev Sea) revealed by high-resolution seismic profiling. In: *System of the Laptev Sea and the adjacent Arctic seas: modern and past environments*. Moscow, pp 332–348 (in Russian)
  40. Rekant PV, Vasiliev AA (2011) Offshore permafrost in the Kara Sea. *Earth's Cryosphere* 15(4):60–62
  41. Rogers JC, Morack JL (1985) Beaufort and Chukchi seacoast permafrost studies. In: *Outer continental shelf environmental assessment program. Final reports of principal investigators*, vol 34. Boulder, Colorado, pp 323–355
  42. Rogers J, Morack J (1980) Geophysical evidence of shallow nearshore permafrost, Prudhoe Bay, Alaska. *J Geophys Res* 85(B9):4845–4853
  43. Romanovskii NN, Hubberten H-W, Gavrilov AV, Tumskoy VE, Tipyenko GS, Grigoriev MN, Siegert C (2000) Thermokarst and land-ocean interactions, Laptev Sea region, Russia. *Permafrost Periglacial Process* 11:137–152

44. Romanovskii NN, Hubberten H-W, Gavrillov AV, Tumskey VE, Kholodov AL (2004) Permafrost of the east Siberian Arctic shelf and coastal lowlands. *Quatern Sci Rev* 23:1359–1369
45. Romanovskiy NN, Hubberten H-W, Gavrillov AV, Eliseeva AA, Tipenko GS (2005) Offshore permafrost and gas hydrate stability zone on the shelf of east Siberian Seas. *Geo-Mar Lett* 25:167–182
46. Shakhova N, Semiletov I, Leifer I, Salyuk A, Rekant P, Kosmach D (2010) Geochemical and geophysical evidence of methane release over the East Siberian Arctic Shelf. *J Geophys Res* 115:C08007. doi:[10.1029/2009JC005602](https://doi.org/10.1029/2009JC005602)
47. Schirrmeyer L, Siegert C, Kuznetsova T, Kuzmina S, Andreev AA, Kienast F, Meyer H, Bobrov A (2002) Paleoenvironmental and paleoclimatic records from permafrost deposits in the Arctic region of Northern Siberia. *Quatern Int* 89:97–118
48. Schirrmeyer L, Grosse G, Schnelle M, Fuchs M, Krubetschek M, Ulrich M, Kunitsky V, Grigoriev M, Andreev A, Kienast F, Meyer H, Babiy O, Klimova I, Bobrov A, Wetterich S, Schwamborn G (2011) Late Quaternary paleoenvironmental records from the western Lena Delta, Arctic Siberia. *Palaeogeogr Palaeoclimatol Palaeoecol* 299:175–196
49. Schwenk T, Spies V, Zuhlsdorff L, Vogt T, Kassens H, Holemann J, Belan A, Rekant P, Gusev E (2005) Imaging submarine permafrost in the Laptev Sea with high-resolution multi-channel seismic data. 2nd European conference on permafrost. 12–16 June 2005, Potsdam, Germany. Abstract
50. Schwamborn G, Rachold V, Grigoriev MN (2002) Late Quaternary sedimentation history of the Lena Delta. *Quatern Int* 89:119–134
51. Sher A (1999) Ice Complex of the Laptev Sea shelf area: paleoecology, age and other problems and current solutions. Quaternary Environment of the Eurasian North (QUEEN). In: Proceedings of the third workshop abstracts, Norway, 16–18 April, Oystese, p 55
52. Slagoda EA (1993) Genesis and microstructure of cryolithogenic deposits of the Bykovsky Peninsula and the Muostakh Island. Ph.D. thesis, Permafrost Institute Yakutsk, RAS Siberian Section (**in Russian**)
53. Soloviev VA, Ginzburg GD, Telepnev EV, Mikhailchuk YuN (1987) Cryotermya and gas hydrates of the Arctic Ocean. Leningrad, *Sevmorgeologia*
54. Taldenkova E, Bauch HA, Stepanova A, Dem'yankov S, Ovsepyan A (2005) Last postglacial environmental evolution of the Laptev Sea shelf as reflected in molluscan, ostracodal and foraminiferal faunas. *Glob Planet Change* 48:223–251
55. Taylor AE (1991) Marine transgression, shoreline emergence—evidence in seabed and terrestrial ground temperatures of changing relative sea levels, Arctic Canada. *J Geophys Res-Solid* 96(B4):6893–6909
56. Tumskey VE (2002) Thermokarst and its role in the development of the Laptev Sea region during the Late Pleistocene and Holocene. Ph.D. Dissertation, Moscow (**in Russian**)
57. Wetterich S, Rudaya N, Tumskey V, Andreev A, Opel T, Schirrmeyer L, Meyer H (2011) Last Glacial Maximum records in permafrost of the East Siberian Arctic. *Quatern Sci Rev* 30:3139–3151
58. Zhigarev LA, Sukhidolskaya LA, Chernyad'ev VP (1982) Cryolithozone of the Arctic seas in Late Pleistocene and Holocene. Moscow